2019 EAGE ANNUAL
81ST CONFERENCE + EXHIBITION
LONDON | THE UNITED KINGDOM

Th_R08_07

Acoustic Land Full Waveform Inversion on a Broadband Land Dataset: the Impact of Optimal Transport

A. Sedova[1]*, J. Messud[1], H. Prigent[1], S. Masclet[1], G. Royle[1], G. Lambaré[1]

[1] CGG

Summary

While there are very few applications of land Full Waveform Inversion (FWI) compared to marine, modern on-shore wide azimuth, dense, broadband acquisition designs offer an outstanding opportunity for FWI application. Several successful examples of acoustic land FWI application to such surveys have been published. The first applications showed the potential of the approach as an early stage velocity model building tool. Later publications demonstrated that acoustic FWI can be used as an efficient model building tool for high resolution velocity models (similar in quality to marine FWI) by investing more effort in dedicated pre-processing and using a two stage workflow based on data selection (Sedova et al., 2017).
We illustrate a new case study based on this workflow. We also demonstrate the impact of optimal transport (OT) FWI on the resulting velocity model, which aims to mitigate cycle skipping. We demonstrate how it corrects several localized failures with conventional FWI and constructs a geologically consistent velocity model.

Introduction

Full waveform inversion (FWI) is a well-established velocity model building tool for marine imaging projects. Applications of FWI to land data are much rarer due to the difficulties associated with elastic effects, near-surface complexities, noise and irregularities in acquisition geometries (Mei et al., 2015). Over the past several years new acquisition designs with full azimuth, dense shooting, long offsets, and broadband vibroseis sources starting as low as 1.5 Hz have offered unrivalled possibilities for FWI applications (Mahrooqi et al., 2012; Baeten et al., 2013). This progress in acquisition design has led to very promising land FWI case studies (Stopin et al., 2014) where diving waves and basic data pre-processing have been used with acoustic FWI. The resulting model corresponded to 6.5 Hz, with higher frequency updates being penalized by the acoustic approximation. Elastic FWI is an obvious solution (Plessix and Solano, 2015) although computational costs remain prohibitive for large full-azimuth surveys. Sedova et al. (2017) demonstrated an improved acoustic FWI workflow applied to Omani broadband full azimuth data leading to a high resolution (HR) acoustic FWI model (13 Hz). The key components of our successful FWI application are dedicated pre-processing and a two-stage workflow where reflected waves are added in the inversion in addition to diving waves during higher frequency iterations. Here, we present a second case study from the Sultanate of Oman, where in addition to the success of a high-resolution (HR) acoustic FWI, we demonstrate that optimal transport (OT) FWI (Poncet et al., 2018) can provide important uplifts in terms of stability, convergence and structural consistency in the high-resolution acoustic FWI result.

FWI application to the Sultanate of Oman data

Our large (about 1000 km^2) broadband full azimuth dataset is formed by merging three separate acquisitions (2014-2016) from the Sultanate of Oman. There are challenges associated with the irregularities in the offset distribution among the merged surveys. The region is known to have a thick sedimentary package in the shallowest 1.5 km, resulting in poor reflection energy and a reduced signal to noise ratio overall. We apply the workflow outlined in Sedova et al. (2017) designed for broadband land data. The first stage consists of inverting diving waves only with dedicated preprocessing of the refraction data which aims to mitigate elastic effects and improves data quality at low frequencies and long offsets. Figure 1 compares results from this first stage (FWI up to 9 Hz) with the velocity model obtained with ray based tomography. The improved focusing and structural simplicity in the migrated stack, as well as the coherency of reflectivity and velocity structures, are clearly visible.

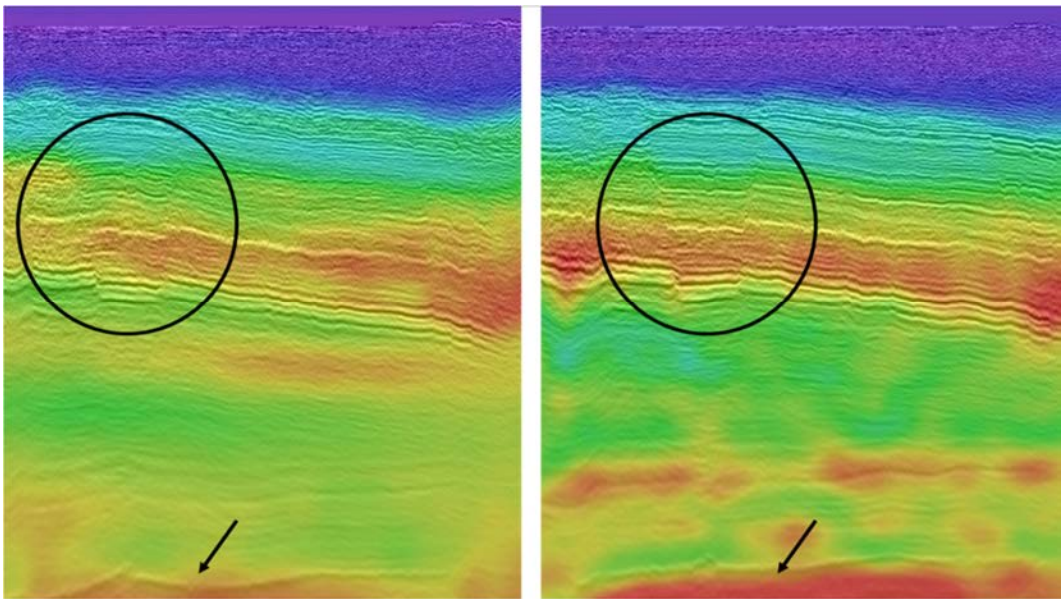

Figure 1: *Velocity model generated by a conventional tomography workflow (left) and the new FWI workflow (right).*

Optimal Transport FWI for cycle skipping issues

While the velocity model was already significantly improved in the first stage, some localized problems were identified. An example is shown in Figure 2 (left) showing a sonic log at a well location. In addition to the fact that the first fast layer is not recovered, the strong velocity inversion is wrongly positioned. These issues could be related to local cycle skipping. Optimal Transport (OT) FWI (Poncet et al., 2018) has been tested and proved to have the capability to overcome this problem. OT implementation in FWI modifies the back-propagated adjoint-source and can be viewed as the result of smart preprocessing of the LSQ residual, enhancing event coherency and low frequencies, and thus the kinematic information (Poncet et al., 2018).
Figure 2 shows on the right that the resulting velocity has a better match with sonic logs and improved consistency with geology.

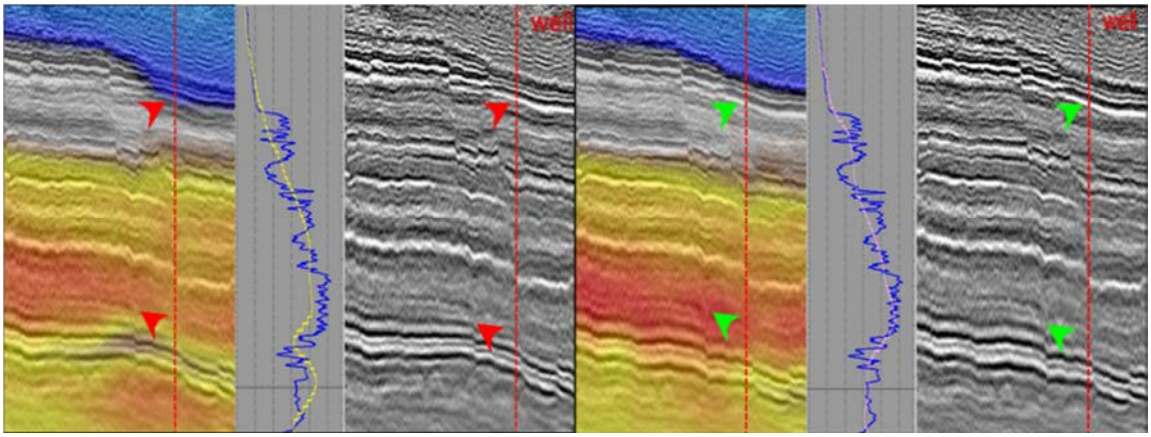

Figure 2: *The results of velocity model building using least-squares FWI (left) and multi-dimensional OT FWI (right) at 9 Hz. Three images are presented for each case correspond to: the velocity model, the velocity profile and sonic log at the well location, and the migrated stack.*

Figure 3 shows an overlay of observed data (in wiggle) and calculated data (in blue white red density) after conventional least square (LSQ) FWI and OT FWI. OT FWI has solved the cycle skipping issues visible with conventional LSQ FWI.

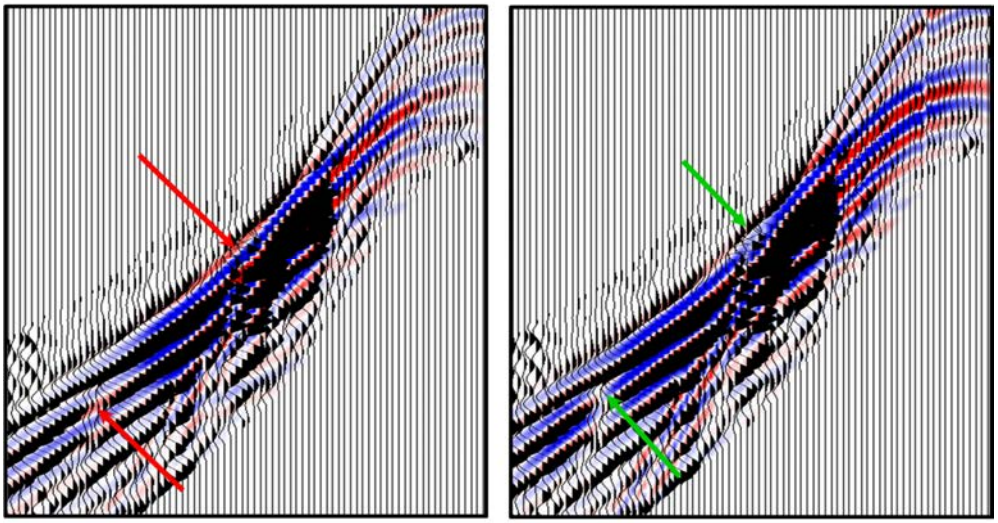

Figure 3: *Real data (wiggle) overlaid on top of synthetics (red-blue) modelled with LSQ FWI (left) and OT FWI (right)*

High resolution land FWI

Finally, following Sedova et al. (2017), we perform the second stage of our FWI workflow. We incorporate reflected waves, processed through the conventional workflow, in addition to diving waves in order to increase the resolution of the velocity model (up to 14 Hz) and to improve the focusing of the migrated image. Figure 4 compares pre-stack depth migrated (PSDM) stacks with the corresponding velocity model after refraction OT FWI (9 Hz) and refraction/reflection FWI (14 Hz). We observe that in the case of refraction/reflection (HR) FWI the velocity model aligns better with the migrated stack.

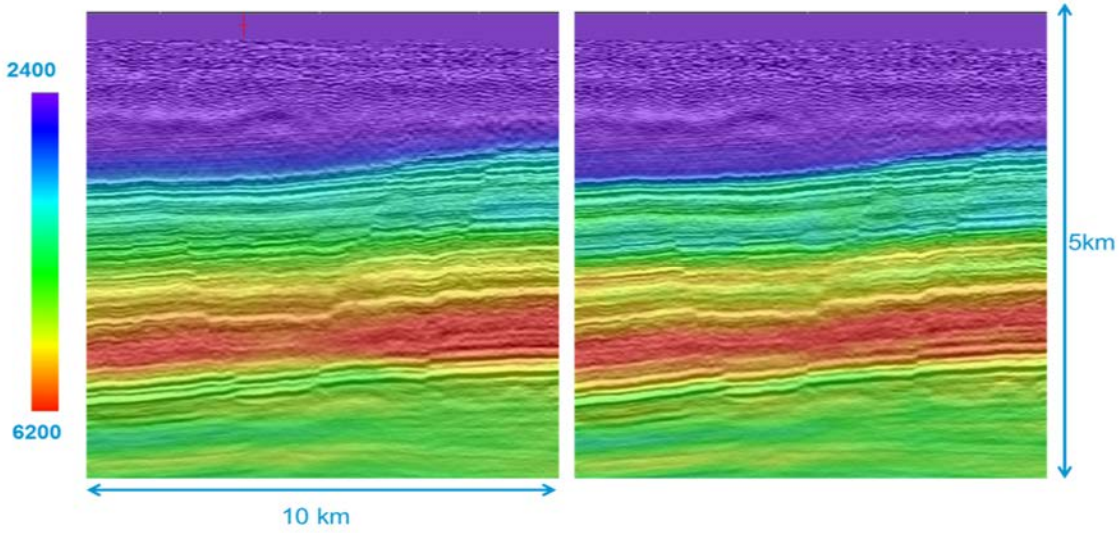

Figure 4: *PSDM stack with overlaid velocity model from refraction OT FWI at 9 Hz (left) and refraction/reflection FWI at 14 Hz (right)*

Figure 5 shows a comparison of snail (pre-stack depth migrated traces sorted by increasing offset and azimuth) common image gathers before and after our second stage of the FWI (9 Hz refraction FWI versus 14 Hz refraction and reflection FWI). We observe that the reflector (indicated by the red arrow) is more coherent after the second stage of FWI. Figure 6 presents a velocity profile at the well location overlaid on the sonic log. The velocity distribution of the refraction/reflection FWI at 14 Hz shows an improved alignment with the sonic log.

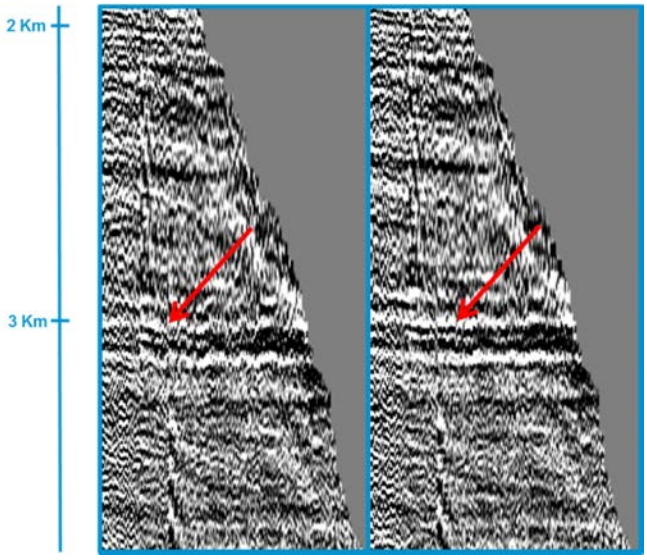

Figure 5: *Snail before (left) and after (right) application of HR FWI at 14 Hz*

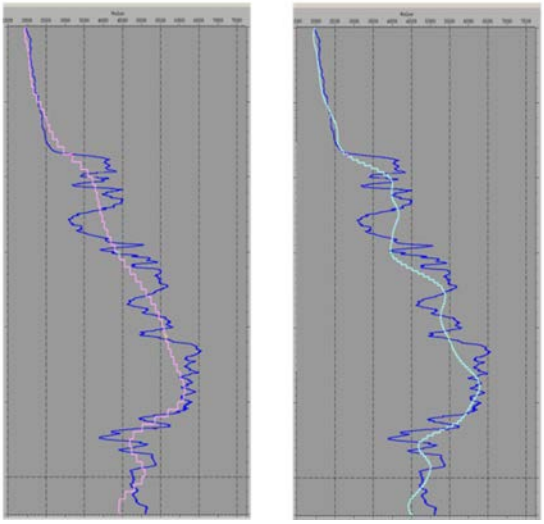

Figure 6: *Velocity profile at well location: refraction OT FWI at 9 Hz (left) and refraction/reflection FWI at 14 Hz (right) overlaid on the sonic log*

In Figure 7 we show depth slices through the velocity model before and after the application of refraction/reflection FWI (up to 14 Hz) on top of the refraction only FWI (9 Hz). We see that our 14 Hz result has recovered the finer structural details of the fault positions.

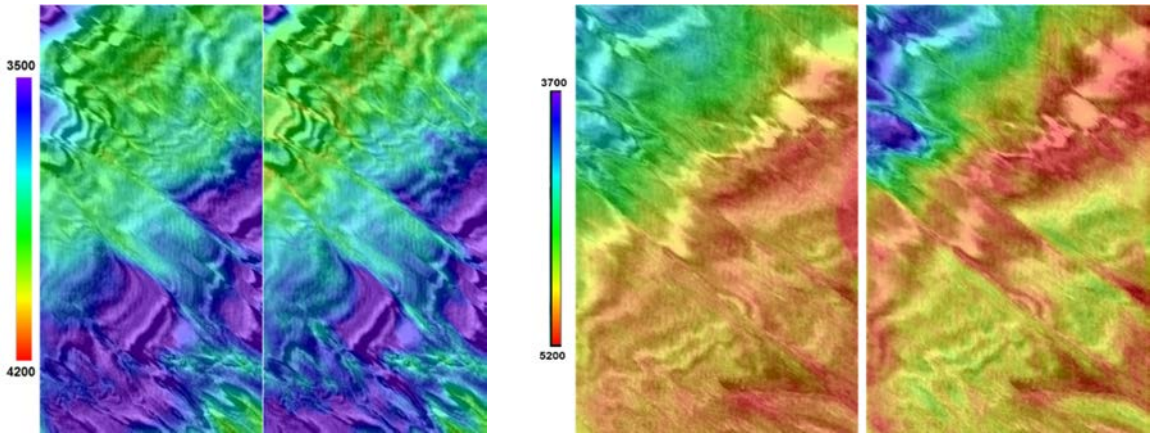

Figure 7: *Depth slices through the velocity model at 1500 m and 2000 m overlaid on PSDM image after refraction OT FWI at 9 Hz (left) and refraction/reflection (HR) FWI at 14 Hz (right).*

Conclusion

We present a new application of the land FWI workflow detailed in Sedova et al. (2017). We show again that the reliable acoustic FWI velocity model could be obtained by application of appropriate refraction/diving wave data preprocessing. In addition we show that OT FWI can stabilize FWI convergence and can provide a more geologically consistent result which aligns with sonic logs. Finally, we show how the incorporation of reflection data dramatically increases subsurface resolution.

Acknowledgements

We are grateful to Occidental Petroleum, PDO and the Ministry of Oil and Gas of the Sultanate of Oman for providing data and permission to present these results.

References

Baeten, G., J.-W. de Maag, R.É. Plessix, R. Klaassen, T. Qureshi, M. Kleemeyer, F. ten Kroode and Z. Rujie [2013] The use of low frequencies in a full-waveform inversion and impedance inversion land seismic case study. *Geophysical Prospecting*, **61**, 701–711.

Mahrooqi, S., S. Rawahi, S. Yarubi, S. Abri, A. Yahyai, M. Jahdhami, K. Hunt, and J. Shorter [2012] Land seismic low frequencies: Acquisition, processing and full wave inversion of 1.5-86 Hz: *82nd Annual International Meeting, SEG*, Expanded Abstracts, 1-5.

Mei, J., Q. Tong [2015] A practical acoustic full waveform inversion workflow applied to a 3D land dynamite survey: *85th Annual International Meeting, SEG*, Expanded Abstracts, 1220-1224.

Plessix, R.É. and C.A.P. Solano [2015] Modified surface boundary conditions for elastic waveform inversion of low-frequency wide-angle active land seismic data: *Geophysical Journal International*, **201**(3), 1324–1334.

Poncet, R., J. Messud, M. Bader, G. Lambaré, G.Viguier, C. Hidalgo [2018] FWI with optimal transport: a 3D implementaion and an application on a field dataset: *80th EAGE Conference and Exhibition, EAGE*, Expanded Abstracts.

Sedova A., G. Royle, O. Hermant, M. Retailleau and G. Lambaré [2017] High-resolution land full-waveform inversion: a case study on a data set from the Sultanate of Oman: *79th Conference and Exhibition, EAGE*, Expanded Abstracts, We A3 04.

Stopin, A., R.É Plessix, and A.A. Said [2014] Multiparameter waveform inversion of a large wide azimuth low-frequency land data set in Oman: *Geophysics*, **79**(3), WA67-WA77.